A trinuclear Pt(II) compound with short Pt–Pt–Pt contacts. An analysis of the influence of π–π stacking interactions on the strength and length of the Pt–Pt bond†

Albert Poater,[a] Silvia Moradell,[b] Elena Pinilla,[c] Jordi Poater,[d] Miquel Solà,*[a] M. Ángeles Martínez*[b] and Antoni Llobet*[e]

Received 5th August 2005, Accepted 21st October 2005
First published as an Advance Article on the web 15th November 2005
DOI: 10.1039/b511625m

In this work we report the first example of a trinuclear Pt(II) complex with Pt–Pt–Pt bonds that are not facilitated by direct intervention of bridging ligands but are partially held by the attractive π–π stacking interaction between the phenyl units of the 4,4′-dimethyl-2,2′-bipyridyl ligands. The effect of the π–π stacking interactions on the strength and length of the Pt–Pt bond has been discussed using reduced models of the interacting moieties in which the aromatic rings have been removed. The nature of the Pt–Pt bonds has been studied through energy decomposition and atoms-in-molecules analyses. The results indicate that the relatively strong (about 40 kcal mol^{-1}) Pt–Pt metallic bond has similar covalent and ionic contributions.

1. Introduction

While extensive studies have been carried out on multinuclear complexes of ruthenium, osmium, rhodium, and iridium, much less work has been devoted to multinuclear platinum or palladium complexes.[1] Furthermore, in most of the known Pd(II) and Pt(II) multinuclear complexes, the metal atoms are held together by bridging ligands, making it unclear whether there is metal–metal bonding or the two metals are held together by the chelating ligands.[2] For instance, a crystal structure for a trinuclear complex of formula [M_3(mercaptonicotinic acid)$_3Cl_3$] (M = Pd(II) and Pt(II)) in which the sulfur atom acts as a bridge between two metal (Pd(II) or Pt(II)) atoms was reported in 1999.[3] Homobinuclear platinum complexes, where a bridging aromatic or iminic ligand separates the platinum centres by at least 5 Å, have been reported too,[1] but in this case the interaction of the two platinum centres takes place *via* its unsaturated π system. Different cases have been described in the literature in which the π–π interaction between the π-conjugated ligands is an important factor in the assemblage of the platinum complexes.[4]

We report here the structural properties of an unexpected trinuclear Pt(II) compound containing the 4,4′-dimethyl-2,2′-bipyridyl ligand. To our knowledge this is the first structure reported for a trinuclear complex of Pt(II) in which intramolecular Pt–Pt–Pt linear contacts are not facilitated by direct intervention of bridging ligands, and with the *trans* disposition for the 2,2′-bipyridine (Bpy) ligand. Although Bpy ligands are commonly used in the formation of different complexes with a great variety of transition metals, the vast majority of metal bis(2,2′-bipyridine) complexes studied by X-ray diffraction possess *cis* geometries.[5–7] Indeed, a general search in the Cambridge Structural Database (CSD) showed that crystal structures of compound type *trans*-M(Bpy)$_2$ are not very common, although some cases are described, mainly for ruthenium.[7,8] However, only a few cases have been described for bis(bipyridine) complexes of d^8 metal ions (Pd(II), Pt(II)) with this unusual form of the *trans* disposition for bipyridine ligands.[9] In addition, both external platinum atoms present *cis*-platinum structures that might be especially appropriate for antitumor purposes.[10] Finally, the role played by the π–π stacking interactions between the π-conjugated ligands in the assemblage of this trinuclear Pt(II) compound have been investigated using reduced models of the interacting moieties.

2. Experimental

All chemicals and reagent-grade products were obtained from Fluka or Aldrich and employed without further purification. The solvents used were purchased from Panreac and SDS (Barcelona, Spain). The ligand 4,4′-dimethyl-2,2′-bipyridyl (4,4′-Me_2Bpy) was obtained from Fluka. The *cis*-dichloro-(1-(carboxylic acid)-1,3-diaminopropane)platinum(II), [$PtCl_2$(Hdab)] was prepared using a method adopted from Moradell *et al.*[11]

2.1. Synthesis

The compound [Pt(Me_2Bpy)$_2$][$PtCl_2$(Me_2Bpy)]$_2$[PF_6]$_2$·2(CH_3)$_2$CO was prepared through an unexpected reaction during addition of Me_2Bpy (22 mg, 0.118 mmol) to a suspension of $PtCl_2$(Hdab) (50 mg, 0.13 mmol) in EtOH–H_2O (3 : 1) (10 ml). The reaction mixture was heated at reflux for 24 h producing an orange solution. Small particles were noted, and the mixture was filtered while it was

[a]*Institut de Química Computacional and Departament de Química, Universitat de Girona, 17071, Girona, Catalonia, Spain. E-mail: miquel.sola@udg.es; Fax: +34-972-418356*
[b]*Departament de Química, Àrea de Química Inorgànica, Facultat de Ciències, Universitat de Girona, 17071, Girona, Spain. E-mail: angeles.martinez@udg.es; antoni.llobet@uab.es*
[c]*Departamento de Química Inorgánica, Facultad de Ciencias Químicas, Universidad Complutense de Madrid, 28040, Madrid, Spain*
[d]*Afdeling Theoretische Chemie, Scheikundig Laboratorium der Vrije Universiteit, De Boelelaan 1083, NL-1081, HV Amsterdam, The Netherlands*
[e]*Departament de Química, Universitat Autònoma de Barcelona, Cerdanyola del Valles, E-08193, Barcelona, Spain. E-mail: antoni.llobet@uab.es; Fax: +34-935-813-101*

† Electronic supplementary information (ESI) available: BP86 optimized *xyz* coordinates of complexes **1** to **3**. See DOI: 10.1039/b511625m

hot. Treatment of the filtered solution with an aqueous solution of NH_4PF_6 produced an orange solid that was filtered off, washed with water and diethyl ether and dried in vacuum. The resulting precipitate was then dissolved in acetone followed by the addition of diethyl ether. After about 1 week, intense orange prisms suitable for X-ray analysis were obtained.

2.2. Structure determination

For $[Pt(Me_2Bpy)_2][PtCl_2(Me_2Bpy)]_2[PF_6]_2\cdot 2(CH_3)_2CO$ the data were collected at room temperature on a Bruker Smart CCD diffractometer, with graphite-monochromated Mo-K_α (λ = 0.71073) radiation, operating at 50 kV and 15 mA. A summary of the fundamental crystal data and refinement data is given in Fig. 1. Data were collected over a hemisphere of the reciprocal space by combination of the three exposure sets. The cell parameters were determined and refined by leasts-squares fit of all reflections collected (θ range = 1.80 to 25.00°, *hkl* from −10, −14, −31 to 10, 13, 34). Each frame exposure time was of 10 s, covering 0.3° in ω. The first 50 frames were re-collected at the end of the data collection to monitor crystal decay. No appreciable drop in the intensities of the standard reflections was observed. Data were corrected for Lorentz and polarization effects but not for absorption.

The structure was solved by Patterson function and conventional Fourier techniques and refined by full-matrix least-squares on F^2.[12] Anisotropic parameters were used in the last cycles of refinement for all non-hydrogen atoms, with the exception of the PF_6 anion and the solvent molecule. For the PF_6 anion, no resolvable positional disorder of the *F* atoms has been found. For this reason, the fluoro atoms were included in two isotropic refinement cycles and their thermal parameters were kept constant in subsequent cycles. Similar treatment has been carried out for the solvent molecule. These facts lead to a maximum shift factor of 1.30 and a highest residual peak in the final difference map of 2.11 e Å^{-3}, both associated with one fluoro atom of the PF_6^- anion. Hydrogen atoms were included in calculated positions and refined riding on their respective carbon atoms with the thermal parameter related to the bonded atoms.[13] The refinement converged to $R_1(F) = 0.055$ [$F^2 > 2\Phi(F^2)$] for 3443 reflections observed and $wR_2(F^2) = 0.1527$ (all data).

Crystal data. $[C_{27}H_{30}Cl_2N_4OPt_{1.5}][PF_6]\cdot(CH_3)_2CO$; formula weight = 935.06; T = 296(2) K; crystal system = monoclinic; space group = $P2(1)/n$; unit cell dimensions = (a = 8.8821(6) Å, b = 12.2768(9) Å, c = 29.030(2) Å, α = 90°, β = 97.235(2)°, γ = 90°); volume = 3140.3(4) Å^3; Z = 4; μ = 6.969 mm^{-1}; reflections collected = 16099; independent reflections = 5513 [R(int) = 0.0713]; final R indices [$I>2\sigma(I)$] = ($R1$ = 0.0551, $wR2$ = 0.1412).

CCDC reference number 281466.

For crystallographic data in CIF or other electronic format see DOI: 10.1039/b511625m

Computational details

The reported calculations have been carried out using the Amsterdam density functional (ADF) package developed by Baerends and coworkers[14] and vectorized by Ravenek.[15] The numerical integration scheme employed has been that of te Velde and Baerends.[16] An uncontracted triple-ς basis set has been used for describing the orbitals of platinum. For carbon, nitrogen, oxygen, and hydrogen, double-ς basis sets have been employed. Both basis sets have been augmented by an extra polarization function.[17] A set of auxiliary s, p, d, f, and g functions, centred in all nuclei, has been introduced in order to fit the molecular density and Coulomb potential accurately in each SCF cycle.[18] Relativistic effects have been included in the energy calculations and geometry optimizations using the ZORA method.[19] This approach gives generally better results than the Pauli formalism. Geometries and energies have been evaluated using a generalized gradient approximation (GGA) that includes a GGA exchange correction of Becke[20] and the GGA correlation correction of Perdew.[21] This method is labelled throughout this work as BP86. The 2002.03 release of the ADF package has been used for all calculations.[22]

We have also carried out an energy decomposition analysis (EDA).[23] In this EDA, the total binding energy (BE) has been divided into deformation energy and interaction energy (BE = ΔE_{def} + ΔE_{int}). The deformation energy (ΔE_{def}) is the energy needed to modify the geometry of the ground state free fragments to attain the geometry that they have in the intermediate. The interaction energy (ΔE_{int}) is the energy released when the two singlet free deformed fragments are brought to the position that they have in the intermediate, and it has been, in turn, split into electrostatic, Pauli repulsion, and orbital interaction terms (ΔE_{int} = ΔE_{elstat} + ΔE_{Pauli} + ΔE_{oi}). The term ΔE_{elstat} corresponds to the classical electrostatic interaction between the unperturbed charge distributions of the prepared fragments and is usually attractive. The Pauli repulsion term, ΔE_{Pauli}, comprises the destabilizing interactions between occupied orbitals and is responsible for the steric repulsion. The orbital interaction term, ΔE_{oi}, accounts for charge transfer (interaction between occupied orbitals on one moiety with unoccupied orbitals of the other, including the HOMO–LUMO interactions) and polarization (empty occupied orbital mixing on one fragment due to the presence of another fragment).[24]

Mayer bond orders have been calculated through the expression:[25]

$$B_{AB}^{Mayer} = \sum_{s}^{\text{on A}} \sum_{t}^{\text{on B}} (PS)_{st}(PS)_{ts} \quad (1)$$

where S is the atomic orbital overlap matrix and P is the density matrix. The sums run over the basis set functions belonging to a given atom A or B.

In addition, local aromaticity changes have been quantified using two probes of local aromaticity based on structure and magnetic properties, respectively. As a structure-based measure of aromaticity, we have employed the harmonic oscillator model of aromaticity (HOMA) index, defined by Kruszewski and Krygowski as:[26]

$$\text{HOMA} = 1 - \frac{\alpha}{n}\sum_{i=1}^{n}(R_{opt} - R_i)^2, \quad (2)$$

where n is the number of bonds considered, and α is an empirical constant (for CC bonds α = 257.7) fixed to give HOMA = 0 for a model non-aromatic system, and HOMA = 1 for a system with all bonds equal to an optimal value R_{opt}, which is 1.388 Å for CC bonds, assumed to be achieved for fully aromatic systems. R_i stands for a running bond length. This index was

found to be one of the most effective structural indicators of aromaticity.[27,28] As a magnetic index of aromaticity, we have used the nucleus-independent chemical shift (NICS) measures proposed by Schleyer and co-workers.[29] This is one of the most widely employed indicators of aromaticity. It is defined as the negative value of the absolute shielding computed at a ring centre or at some other interesting point of the system. Rings with large negative NICS values are considered aromatic. The more negative the NICS values, the more aromatic the rings are. The GIAO method[30] was used to perform calculations of NICS at ring centres (NICS(0)) determined by the non-weighted mean of the heavy atoms coordinates.

Finally, an atoms in molecules (AIM)[31] analysis has been carried out by means of the AIM2000 program.[32] Topological properties of the electron density at the bond critical points (BCP) of the Pt–Pt interactions were analyzed. For the AIM analysis and NICS calculations, the wave function was computed at the BP86 level of theory with the GAUSSIAN03 package[33] using the ADF optimized geometries. The Pt atoms were represented with relativistic effective core pseudo-potentials (RECP) and the associated basis set[34] augmented with a polarization function (α = 0.993, Pt).[35] The remaining atoms (C, H, N, O, and Cl) were represented with the 6-31G(d,p) basis set.[36]

3. Results and discussion

3.1. Molecular and electronic structure

The X-ray single crystal structure analysis shows that the compound $[Pt(Me_2Bpy)_2][PtCl_2(Me_2Bpy)]_2[PF_6]_2\cdot 2(CH_3)_2CO$ forms a tris-platinum species that crystallises in the monoclinic space group $P2(1)/n$ with $Z = 4$. This species has several equivalent atoms because of the inversion centre. The ORTEP[37] diagram is depicted in Fig. 1 with selected bond lengths and angles.

Compound **1** {$[Pt(Me_2Bpy)_2][PtCl_2(Me_2Bpy)]_2[PF_6]_2\cdot 2(CH_3)_2$-CO} described in this work consists of two neutral $[PtCl_2(Me_2Bpy)]$ molecules alternatively stacked with one cationic $[Pt(Me_2Bpy)_2]^{2+}$ moiety, resulting in intramolecular Pt–Pt–Pt linear contacts with a distance of 3.474(6) Å between the adjacent Pt(II) atoms. The existence of M–M contacts between square-planar complexes of Pt(II) in the range 2.7 Å $< d >$ 3.5 Å, shorter than the van der Waals sum, is well-known in the crystal structures of dimers and chains.[1,2,38–41] In our case, the 3.474(6) Å of the Pt–Pt separation between adjacent entities is similar to those reported for the red form of $PtCl_2(Bpy)$ (Bpy = 2,2′-bipyridine) (3.449(1) Å), in which the square-planar complexes stack to form an approximately linear Pt–Pt chain with a spacing of 3.449(1) Å.[40,42]

As is known in most of the reported cases with complexes of platinum(II),[43] the coordination of each platinum is approximately square planar, but there is a substantial distortion induced by the bidentate ligand that forms a five-membered chelate ring with the Pt atom. The deviations from ideal 90° bond angles, which decrease to 78.7(4)° in the N(1)–Pt(1)–N(2) bond angle and to 80.6(4)° in the N(3)–Pt(2)–N(4) bond angle, may be attributed to a chelate effect. The N–Pt–N chelate angles within each moiety are not identical. This suggests that, in the cationic $[Pt(Me_2Bpy)_2]^{2+}$ moiety, the bipyridine ligands are considerably more sterically crowded within the coordination sphere and are forced towards a smaller N–Pt(1)–N bond angle. For the charged $[Pt(Me_2Bpy)_2]^{2+}$ central fragment, it is interesting to note, as shown in Fig. 1, that two bipyridine ligands are placed in mutually *trans* position in an inversion centre arrangement around the Pt(1) atom. For the neutral $[PtCl_2(Me_2Bpy)]$ entities, the Cl(1)–Pt(2)–Cl(2) (89.72(13)°), N(3)–Pt(2)–N(4) (80.6(4)°) and N(3)–Pt(2)–Cl(1) (175.5(3)°) bond angles are similar to those reported for the yellow form of $PtCl_2(Bpy)$.[40] The Pt(2)–Cl distances (Pt(2)–Cl(1) = 2.294(4) Å and Pt(2)–Cl(2) = 2.290(3) Å) are similar to those observed for the yellow polymorph too; however the Pt–N bond lengths (Pt(2)–N(3) = 1.990(11) Å, Pt(2)–N(4) = 1.998(10) Å) are somewhat shorter than those found for other Pt(II) compounds.[44] In contrast, all four Pt–N bond distances (Pt(1)–N(1) = 2.021(10) Å and Pt(1)–N(2) = 2.017(10) Å) for the cationic $[Pt(Me_2Bpy)_2]^{2+}$ entity are similar to those found in other similar complexes of platinum(II).[44–46]

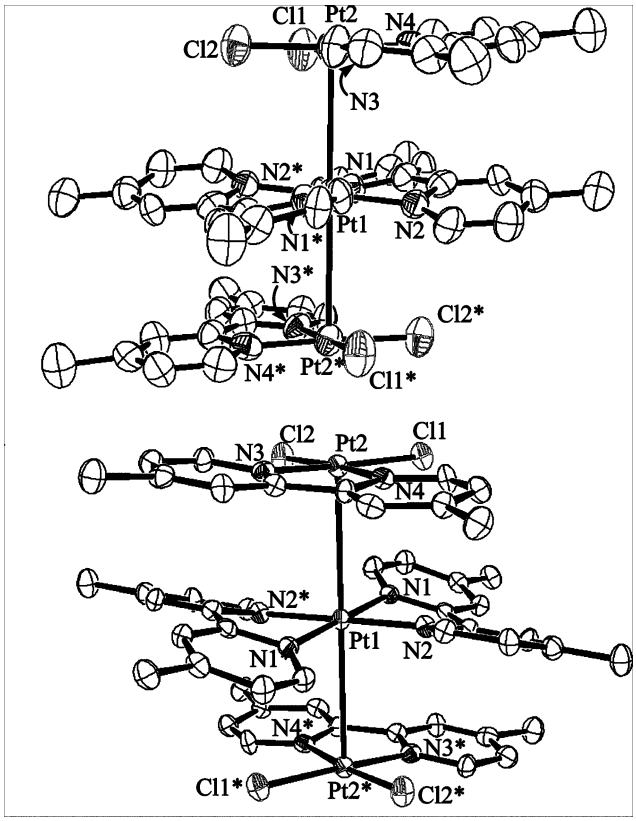

Fig. 1 Views of the trinuclear $[Pt(Me_2Bpy)_2][PtCl_2(Me_2Bpy)]_2[PF_6]_2\cdot 2(CH_3)_2CO$. Distances in Å and angles in °: Pt(2)–Cl(1) = 2.294(4), Pt(1)–Pt(2) = 3.4745(6), Pt(1)–Pt(2)–Pt(3) = 180.000(17), N(1)–Pt(1)–N(2) = 78.7(4), Pt(2)–Cl(2) = 2.290(3), Pt(1)–N(2) = 2.017(10), Cl(1)–Pt(1)–Cl(2) = 89.72(13), Cl(1)–Pt(2)–N(3) = 175.5(3), Pt(2)–N(3) = 1.990(11), Pt(1)–N(1) = 2.021(10), N(3)–Pt(2)–N(4) = 80.6(4), Pt(2)–Pt(1)–N(2) = 89.7(3), Pt(2)–N(4) = 1.998(10), Cl(1)–Pt(2)–N(4) = 95.8(3), Cl(2)–Pt(2)–N(4) = 174.2(3).

To get further insight into the structure of this complex, DFT calculations have been performed. The optimized structure is depicted in Fig. 2a. The Pt–Pt distance in this BP86 optimized structure of 3.184 Å is shorter than the experimental one by 0.290 Å, with a relative error of about 9%. The energetic cost of increasing the Pt–Pt distance by 0.290 Å while keeping the rest of the geometrical parameters fixed in the optimized BP86 complex

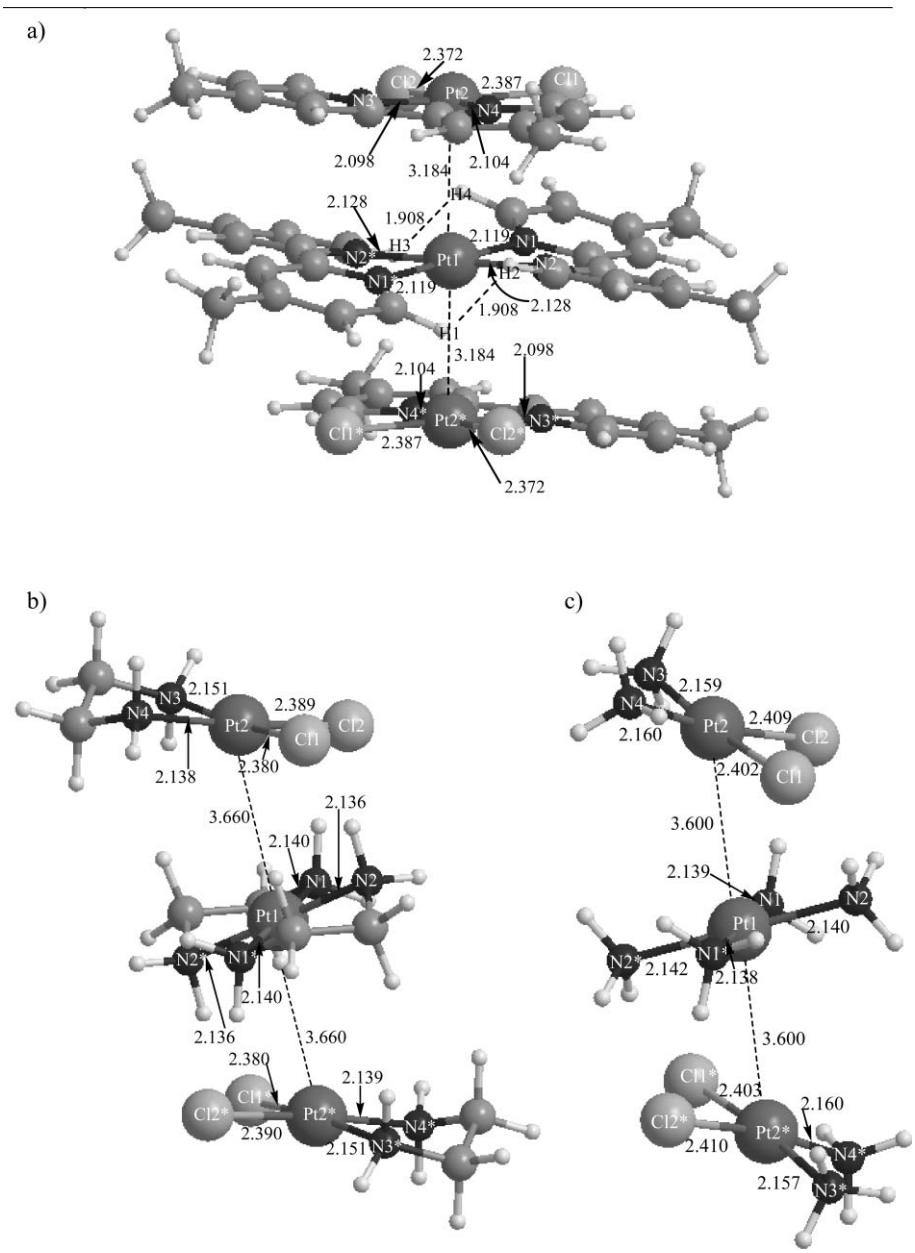

Fig. 2 BP86 optimized geometries of complexes (a) **1** $\{[Pt(Me_2Bpy)_2][PtCl_2(Me_2Bpy)]_2\}^{2+}$, (b) **2** $\{[Pt(en)_2][PtCl_2(en)]_2\}^{2+}$, and (c) **3** $\{[Pt(NH_3)_4][PtCl_2(NH_3)_2]_2\}^{2+}$. Distances in Å and angles in degrees.

is 7.6 kcal mol^{-1}, that is, the elongation of a single Pt–Pt bond by 0.290 Å in this complex costs 3.3 kcal mol^{-1}. Moreover, reoptimization of the geometry should reduce this value. This shows that the Pt–Pt bond is quite flexible in this molecule. The error in the optimized BP86 Pt–Pt bond length cannot be attributed to the difficulty of generalized gradient approximation (GGA) density functionals for describing π–π stacking interactions because GGA functionals tend to underestimate these interactions.[47] Neither it can it be ascribed to a failure in the description of the metal–metal interaction because GGA functionals including relativistic effects describe correctly this kind of interaction.[48] Rather, the error in the theoretical determination of the Pt–Pt bond distance may be the result of packing effects facilitated by a loose Pt–Pt bond. Nevertheless, the possibility that the theoretical study of the present complex requires the use of more sophisticated theoretical methods such as the multireference CI methodologies cannot be ruled out, especially if one takes into account the low HOMO–LUMO gap found for this system (*vide infra*). Unfortunately, these methodologies are currently unaffordable for computing large systems such as the present complex.

The Pt–Cl calculated distances are slightly larger (2.387 Å and 2.372 Å) than in the X-ray structure (2.294 Å and 2.290 Å), and the same happens with the Pt–N ones that present values of 2.098 Å and 2.104 Å for both external platinum atoms, and 2.119 Å and 2.128 Å for the central one. As a consequence of the *trans*-influence of the chlorine anions, it is found that the shorter the Pt–Cl bond distance, the larger the Pt–N bond length for the ligand placed in *trans*-position. It is worth noting that the distances between

the external pairs of faced hydrogen atoms (H1–H2 and H3–H4 in Fig. 2a) of the two Me_2Bpy ligands in the central charged entity are 1.908 Å, 0.152 Å shorter than 2.060 Å, the value corresponding to the H1–H2 distance in the optimized geometry of the free charged $[Pt(Me_2Bpy)_2]^{2+}$ entity. The presence of these repulsive interactions explains the distortion of the Bpy ligands out of the molecular plane.

To discuss the π–π stacking effect in the aromatic rings of the Me_2Bpy units, the Me_2Bpy ligands were substituted by ethylendiamines to yield complex **2**. Then, the Me_2Bpy units were replaced by simple amine units (complex **3**) to assess the effect of having a fixed N–Pt–N bite angle in bidentate ligands, as in complexes **1** and **2**. In both simulated complexes an important elongation of the Pt–Pt bond distances took place achieving values of 3.600 Å and 3.660 Å, respectively, confirming that π–π stacking interactions play a significant role on the Pt–Pt bond lengths. Indeed, comparing our experimental results with the reported $[Pt(CN)_4]^{2-}$ chain,[49] we found stronger interactions between the platinum atoms in complex **1** thanks, in part, to the favourable π–π stacking effect of the pyridine units not present in the $[Pt(CN)_4]^{2-}$ chain. Fig. 2 shows the three calculated structures for complexes **1** to **3**. The BP86 optimized *xyz* coordinates are given as ESI.†

The charged square planar central $[Pt(Me_2Bpy)_2]^{2+}$ moiety in **1** is not perfectly planar due to the fact that the Me_2Bpy units suffer in-plane and bow distortions.[50] The in-plane effect can be described by the angle θ_P depicted in Fig. 3a. This angle is near 170° for both the calculated species and the X-ray data for the central charged entity and only slighty smaller for each external neutral entity. The similarity between all these values reflects the fact that it is the size of the metal, the platinum in this case, which is the main factor that determines this in-plane effect. On the other hand, the so-called bow distortion[5] is the deformation of the Bpy ligand that allows the coordination of the two Bpy units at a single platinum atom in a *trans* disposition. This bow distortion allows the formation of the complex because without this effect the insertion of two Me_2Bpy units at a single platinum atom would not be possible. This distortion, measured by the angle θ_B depicted in Fig. 3b, is different for the central and external

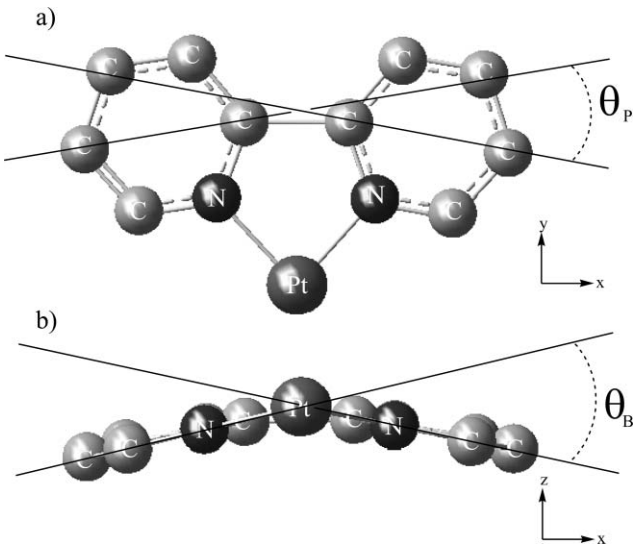

Fig. 3 Schematic representation of (a) in-plane and (b) bow distortion.

units: 18.2° (exp. 20.6°) and 12.1° (exp. 9.8°), respectively. For the BP86 optimized free central charged $[Pt(Me_2Bpy)_2]^{2+}$ and external neutral $[Pt(M_2Bpy)Cl_2]$ moieties the θ_B values are 21.4° and 4.3°, respectively. Thus, there is a slight decrease in the bow distortion when going from the free central charged fragment to complex **1** and a remarkable increase for the free external neutral moieties. These changes in the bow angles, which are energetically not very demanding (*vide infra*), help to reduce steric repulsion between the external and the central moieties while at the same time favour the π–π stacking interactions. Indeed, the angle between the central metallic entity and the external metallic entities of **1** is only 7.4° (exp. 6.7°) (this angle corresponds to the angle between the best fitted planes defined by each metal and the four atoms of the ligands bonded to it). This angle increases to 35.8° for **2** and nearly 40° for **3**. In all the complexes the angle between the two external metallic entities is close to zero.

The HOMO–LUMO gap is extremely low for complex **1** (27.5 kcal mol^{-1}) and somewhat larger for complexes **2** (48.1 kcal mol^{-1}) and **3** (53.0 kcal mol^{-1}). Frontier orbitals (see Fig. 4) are more stable in **2** and **3** as compared to **1**. The HOMO orbitals are mainly based on d_{z^2} contributions of the three metals, through an antibonding interaction. As can be seen in Fig. 4,[51] the larger overlap between atomic Pt d_{z^2} orbitals in complex **1** because of the shorter Pt–Pt bond distances explains its higher HOMO energy. Although the LUMO orbital is slightly different for each calculated complex, it is always related to the Pt–X bonds. The LUMO in complex **1** is mainly located on the central metallic entity, while those of complexes **2** and **3** have larger components on the external metallic units. Finally, the central metal presents a similar Mulliken charge for the three calculated structures (0.88 e in **1**, 0.88 e in **2**, and 0.86 e in **3**), but the external platinum atoms display some differences, thus, in species **1** the external Pt atom presents higher positive Mulliken charges (0.62 e) than for **3** (0.56 e) and **2** (0.54 e) systems.

3.2. The nature of the Pt–Pt bonds

To discuss the nature of the Pt–Pt chemical bonding and to quantify the degree of ionicity or covalency of the Pt–Pt bonds, a bond energy decomposition analysis (EDA) has been carried out. We have divided complexes **1–3** into two fragments: an external neutral $[PtCl_2X]$ moiety and the rest of the molecule. The results are summarized in Table 1.

It is found that the binding energy (BE) of the Pt–Pt bond of the two fragments considered does not change significantly (around 43 kcal mol^{-1}) with the substitution of the ligands in spite of the large differences in the Pt–Pt bond lengths. This is apparently in contradiction with the fact that π–π stacking in complex **1** favours the formation of the Pt–Pt bond and one should expect a larger BE for complex **1** than for **2** or **3**. The reason for this discrepancy can be found in the distortion suffered by complexes **2** and **3** that brings the chlorine substituents of the Pt2 and Pt2* groups closer

Table 1 Energy decomposition analysis (EDA). Energies in kcal mol^{-1}

Compound	ΔE_{Pauli}	ΔE_{elstat}	ΔE_{oi}	ΔE_{def}	BE	Covalency (%)
1	52.9	−53.3	−45.4	2.3	−43.5	46.0
2	38.0	−43.9	−46.4	8.3	−43.9	51.4
3	34.8	−49.3	−39.7	11.7	−42.5	44.6

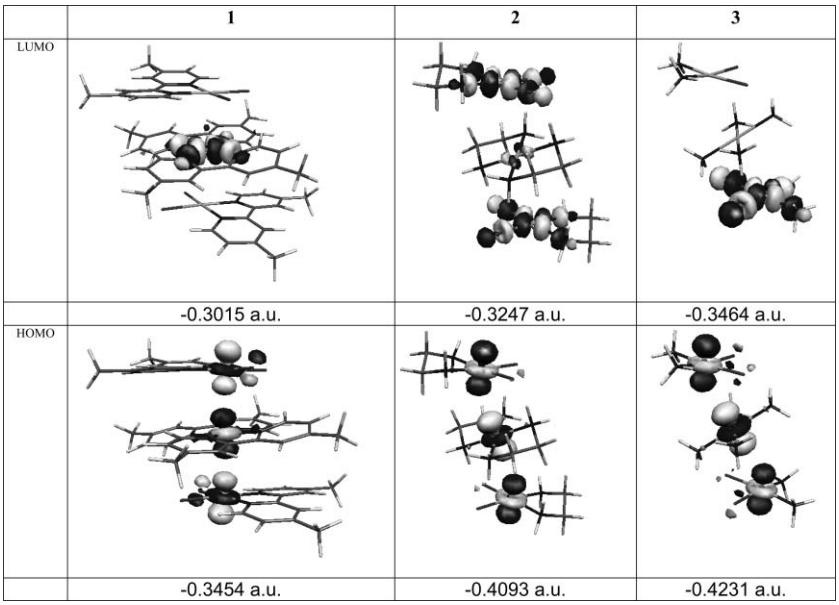

Fig. 4 HOMO and LUMO molecular frontier orbitals for complexes **1**, **2**, and **3**. Isosurface values are −0.05 a.u. and 0.05 a.u.

to the central complex Pt1. This kind of distortion allows the formation of hydrogen bonds between the amine hydrogen atoms and the chlorine groups in complexes **2** and **3**. These hydrogen bonds, not present in complex **1**, have an important influence in the calculation of the BE for complexes **2** and **3**. To demonstrate this hypothesis, we have reoptimized complex **2** keeping all Cl–Pt–Pt and N–Pt–Pt angles to 90° and the Pt2–Pt1–Pt2* angle to 180° (the optimized *xyz* coordinates of this model are given in the ESI†). The Pt–Pt BE for this new constrained species is reduced by about 9.0 kcal mol^{-1} as compared to that of the free complex **2**, due to the partial loss of H-bonding interactions. Thus, in the absence of H-bonding interactions, the BE of complex **1** is significantly larger than that of complex **2**, showing that π–π stacking interactions have a remarkable effect both on the Pt–Pt bond length and strength.

The BE is the sum of the interaction energy and the deformation energy. The latter is especially low for the molecules that present bidentate amines, and even lower if there are aromatic systems attached to the nitrogen atoms (11.7 kcal mol^{-1} for **3**, 8.3 kcal mol^{-1} for **2**, and 2.3 kcal mol^{-1} for **1**), perhaps due to a lower flexibility of the bidentate ligands that does not allow for big rearrangements of the coordination sphere of the metal. The Pauli repulsion is higher for **1** (52.9 kcal mol^{-1}) than for **3** (34.8 kcal mol^{-1}) and **2** (38.0 kcal mol^{-1}) as expected from the shorter Pt–Pt bond distances and the size of the ligands in **1**. Not unexpectedly, the electrostatic interaction between the charged $[[Pt(Me_2Bpy)_2][PtCl_2(Me_2Bpy)]_2]^{2+}$ and the neutral $[PtCl_2(Me_2Bpy)]$ fragments is in absolute value larger for the complex having the shortest Pt–Pt distance. Thus, the electrostatic component, related to the ionic character of the bond, is more stabilizing for complex **1** (−53.3 kcal mol^{-1}) than for **3** (−49.3 kcal mol^{-1}) and **2** (−43.9 kcal mol^{-1}). Finally, the orbital component is more negative for **2** (−46.4 kcal mol^{-1}) and **1** (−45.4 kcal mol^{-1}) than for **3** (−39.7 kcal mol^{-1}), thus indicating that the covalent character of the Pt–Pt interactions is favoured in bidentate ligands. The ionic character of the Pt–Pt interaction (measured as $[\Delta E_{elstat}/(\Delta E_{elstat} + \Delta E_{oi})] \times 100$) is quite important in **1** (54.0%), but similar to that of **3** (55.4%), and not far from **2** (48.6%).

Table 2 Mayer bond orders for the BP86 optimized complexes **1–3**

Compound	Pt–Pt	Pt–Cl	Pt–N (external metallic unit)	Pt–N (central metallic unit)
1	0.15	0.72	0.41	0.44
2	0.07	0.71	0.35	0.38
3	0.07	0.69	0.34	0.37

To further examine the nature of the Pt–Pt bond, we have computed the Mayer bond orders (MBO)[25] for complexes **1–3** (see Table 2). The values of Pt–Pt MBOs are relatively low, even for metal–metal bonds that are usually associated with small MBOs.[52] This result shows that the electron sharing between the two Pt atoms is particularly low. Complex **1** with a value of 0.15 presents the largest Pt–Pt MBO in agreement with this complex having the shortest Pt–Pt distance. The Pt–Cl and Pt–N bond orders are similar for all the studied species.

More information on the Pt–Pt interaction can be achieved from an atoms in molecules (AIM)[31] analysis. In the AIM analysis, topological properties of the electron density (ρ(r)) are analyzed to define the type of interaction between bonding atoms. A chemical bonding is characterized by the bond critical point (BCP), defined by the AIM theory as the point where ρ(r) becomes a minimum value along the bond path. Table 3 summarizes the BCP properties of these Pt–Pt interactions for complexes **1–3**.

Table 3 BCP properties of the Pt–Pt interactions, in a.u

Compound	ρ_{Pt-Pt}	$\nabla^2\rho_{Pt-Pt}$	H_{Pt-Pt}
1	0.0258	−0.0160	−0.0010
2	0.0125	−0.0059	−0.0002
3	0.0133	−0.0069	−0.0001

The first property of interest is the electron density at the BCP (ρ_{BCP}(Pt–Pt)), which is related to the strength of the interaction. For the three cases, values of ρ_{BCP}(Pt–Pt) are within the range 0.013–0.026 a.u., with compound **1** presenting the highest ρ_{BCP}(Pt–Pt) in line with the Pt–Pt bond being the shortest for this complex. These ρ_{BCP}(Pt–Pt) values are much lower than for a normal covalent bond[53] but significantly higher than the practical boundary of a molecule ($\rho \approx 0.001$ a.u.), and quite similar to that of typical hydrogen bonds ($\rho_{H\text{-}bond} \approx 0.002$–$0.040$ a.u.).[53,54] Although ρ_{BCP} for metal–metal bonds is usually small, the ρ_{BCP}(Pt–Pt) is particularly low in line with the small MBO values found for the Pt–Pt interactions. Another important property is the Laplacian of the electron density at the BCP ($\nabla^2\rho_{Pt\text{–}Pt}$), which represents the curvature of the electron density in three-dimensional space at the BCP of the Pt–Pt interaction. In general, a negative value of $\nabla^2\rho$ indicates that the electron density is locally concentrated, while a positive value means that ρ is locally depleted. Therefore, a negative value of $\nabla^2\rho$ at the BCP is indicative of a dominant character of the open-shell (covalent) interactions, whereas a positive value of $\nabla^2\rho$ is related to closed-shell (electrostatic) interactions. From the results of $\nabla^2\rho_{Pt\text{–}Pt}$ in Table 3, it can be seen that in all three cases the Pt–Pt interactions present values for $\nabla^2\rho_{Pt\text{–}Pt}$ close to zero, quite common for metal–metal bonds for which neither the covalent nor the electrostatic interactions are favored.[52] The above information extracted from the Laplacian is corroborated by means of the total energy density (H) at the BCP.[55] H is the sum of the electronic kinetic energy density (G) and the electronic potential energy density (V). Thus, a covalent interaction is characterized by a negative value of H, whereas an electrostatic one is characterized by a positive H value. The negative but close to zero values of $H_{Pt\text{–}Pt}$ in Table 3 are usual in metal–metal interactions[52] and are indicative of similar ionic and covalent contributions. Thus, from the EDA and AIM analysis, it can be concluded that the Pt–Pt bond is a metallic bond of intermediate strength and with similar ionic and covalent contributions.

Finally, because of the importance of the π–π stacking interactions in complex **1**, we have decided to analyze the changes in local aromaticity of the aromatic six-membered rings (6-MRs) when complex **1** is formed from the $[PtCl_2(Me_2Bpy)]$ and $[Pt(Me_2Bpy)_2]^{2+}$ fragments by means of the HOMA and NICS indices. The results are listed in Table 4. We have taken as a reference the values for the free Me_2Bpy ligand (HOMA = 0.979 and NICS = −6.6 ppm) that have been compared with those of complex **1** and the corresponding free $[PtCl_2(Me_2Bpy)]$ and $[Pt(Me_2Bpy)_2]^{2+}$ fragments. Going from the Me_2Bpy ligand to the $[PtCl_2(Me_2Bpy)]$ and $[Pt(Me_2Bpy)_2]^{2+}$ fragments there is an almost insignificant reduction of aromaticity that must be attributed to the in-plane and bow distortions due to coordination of the Me_2Bpy ligands to the metal atoms. These distortions are more important in the $[Pt(Me_2Bpy)_2]^{2+}$ fragment (*vide supra*) and also the reduction in local aromaticity is somewhat more important in this particular fragment. However, in general, local aromaticity changes are very small as expected from the well-known fact that small distortions of the aromatic rings results in essentially unperturbed local aromaticities.[56] Changes in local aromaticity of the 6-MRs measured by HOMA when going from free $[PtCl_2(Me_2Bpy)]$ and $[Pt(Me_2Bpy)_2]^{2+}$ fragments to complex **1** are also very small, especially for the neutral $[PtCl_2(Me_2Bpy)]$ fragment. For the central charged $[Pt(Me_2Bpy)_2]^{2+}$ fragment there is some increase in local aromaticity as expected from the aforementioned reduction in the bow angle for this fragment in complex **1**. Finally, the significant increase in local aromaticity when going from the free fragments to complex **1** given by NICS is likely an artifact of the NICS indicator of aromaticity caused by the magnetic couplings between superimposed 6-MRs.[56a] Nevertheless the increase in the NICS values of the N3–N3* rings and especially the N1–N1* rings is clearly another strong argument in favour of the π–π stacking interactions between the pairs of N1–N3* and N1*–N3 rings. As a whole, while π–π stacking interactions are important in the formation of the Pt–Pt bond in complex **1**, aromaticity changes have likely an almost irrelevant influence.

Table 4 HOMA and NICS (in ppm) local aromaticity indices. Labels of aromatic rings are those in Fig. 2

Aromatic ring	HOMA	NICS
Me_2Bpy	0.979	−6.6
N3–N3*	0.976	−6.3
N4–N4*	0.975	−6.0
N2–N2*	0.980	−6.1
N1–N1*	0.982	−6.7
N3–N3* $[PtCl_2(Me_2Bpy)]$	0.978	−5.6
N4–N4* $[PtCl_2(Me_2Bpy)]$	0.975	−5.6
N2–N2* $[Pt(Me_2Bpy)_2]^{2+}$	0.971	−5.5
N1–N1* $[Pt(Me_2Bpy)_2]^{2+}$	0.972	−5.5

4. Conclusions

The characterization of the new trinuclear $[[Pt(Me_2Bpy)_2]\text{-}[PtCl_2(Me_2Bpy)]_2]^{2+}$ complex **1** through X-ray data has been accomplished. This interesting complex presents short Pt–Pt contacts that indicate the presence of metal–metal bonds. Comparison between complexes **1**, **2**, and **3** suggests that the π–π stacking interactions between the pyridine units are responsible, in part, for the short Pt–Pt distances found in complex **1**. The Pt–Pt bond has an intermediate strength with a binding energy of about 40 kcal mol^{-1}. As to the nature of the Pt–Pt interaction, this is a metallic bond with both covalent and electrostatic components being almost equally important as derived from the AIM and EDA analyses.

Acknowledgements

This research has been financed by MCYT of Spain through the projects BQU2000-0458, BQU2003-02884, and BQU2002-04112-C02-02. AL and MS are grateful to CIRIT Generalitat de Catalunya (Spain) for the Distinction award and AL for the aid SGR2001-UG-291. AL also thanks Johnson Matthey for a K_2PtCl_4 loan. AP thanks Dr C. Bo and Dr J. M. Campanera for helpful comments related to AIM and MBO, respectively. AP and SM are grateful for the award of a doctoral grant from MEC and UdG respectively. The authors thank one of the referees for valuable suggestions.

References

1 A. Klein, *Reviews in Inorganic Chemistry*, 2000, **20**, 283–303.
2 J. J. Novoa, G. Aullón, P. Alemany and S. Álvarez, *J. Am. Chem. Soc.*, 1995, **117**, 7169–7171.

3 S. Marchala, V. Moreno, G. Aullón, S. Álvarez, M. Quirós, M. Font-Bardia and X. Solans, *Polyhedron*, 1999, **18**, 3675–3682.
4 M. Kato, M. Kozakai, C. Fukagawa, T. Funayama and S. Yamauchi, *Mol. Cryst. Liq. Cryst.*, 2000, **343**, 35–40.
5 A. Hazell, *Polyhedron*, 2004, **23**, 2081–2083.
6 M. Bakir, S. Paulson, P. Goodson and B. P. Sullivan, *Inorg. Chem.*, 1992, **31**, 1129–1135.
7 A. W. Cordes, B. Durham, P. N. Swepston, W. T. Pennington, S. M. Condren, R. Jensen and J. L. Walsh, *J. Coord. Chem.*, 1982, **11**, 251–260.
8 (*a*) B. Durham, S. R. Wilson, D. J. Hodgson and T. J. Meyer, *J. Am. Chem. Soc.*, 1980, **102**, 600–607; (*b*) N. R. Weathers, R. C. Sadoski, B. Durham and A. W. Cordes, *Acta Crystallogr., Sect. C*, 1997, **53**, 1047–1049; (*c*) B. J. Coe, T. J. Meyer and P. S. White, *Inorg. Chem.*, 1993, **32**, 4012–4020; (*d*) T. Togano, H. Kuroda, N. Nagao, Y. Maekawa and H. Nishimura, *Inorg. Chim. Acta*, 1992, **196**, 57–63; (*e*) H. Nagao, H. Nishimura, H. Funato, Y. Ichikawa, F. S. Howell, M. Mukaida and H. Kakihana, *Inorg. Chem.*, 1989, **28**, 3955–3959; (*f*) R. Kroener, M. J. Heeg and E. Deutsch, *Inorg. Chem.*, 1988, **27**, 558–566; (*g*) A. J. Blake, A. McA. Marr, D. W. H. Rankin and M. Schröder, *Acta Crystallogr., Sect. C*, 1988, **44**, 935–936.
9 (*a*) A. Hazell and A. Mukhopadhyay, *Acta Crystallogr., Sect. B*, 1980, **36**, 1647–1649; (*b*) A. W. Cordes, B. Durham, P. N. Swepston, W. T. Pennington, S. M. Condren, R. Jensen and J. L. Walsh, *J. Coord. Chem.*, 1982, **11**, 251–260.
10 (*a*) C. Molenaar, J.-M. Teuben, R. J. Heetebrij, H. J. Tanke and J. Reedijk, *JBIC, J. Biol. Inorg. Chem.*, 2000, **5**, 655–665; (*b*) K. Charalabopoulos, S. Karkabounas, E. Loachim, V. Papalimneou, K. Syrigos, A. Evangelou, N. Agnantis and N. Hadjiliadis, *Eur. J. Clin. Invest.*, 2002, **32**, 129–133; (*c*) B. Lippert, *Coord. Chem. Rev.*, 1999, **182**, 263–295; (*d*) L. R. Kelland and N. P. Farrel (Editors), *Platinum-Based drugs in Cancer Therapy*, Humana Press, Totowa, 2000; (*e*) J. Reedijk, *Proc. Natl. Acad. Sci. USA*, 2003, **100**, 3611–3616.
11 S. Moradell, J. Lorenzo, A. Rovira, M. S. Robillard, F. X. Avilés, V. Moreno, R. Llorens, M. A. Martínez, J. Reedijk and A. Llobet, *J. Inorg. Biochem.*, 2003, **96**, 493–502.
12 G. M. Sheldrick, *SHELX97 [Includes SHELXS97, SHELXL97, CIFTAB]-Programs for Crystal Structure Analysis (Release 97-2)*, University of Göttingen, Germany, 1998.
13 G. M. Sheldrick, *Program for Refinement of Crystal Structures*, University of Göttingen, Germany, 1997.
14 (*a*) E. J. Baerends, D. E. Ellis and P. Ros, *Chem. Phys.*, 1973, **2**, 41–51; (*b*) C. Fonseca Guerra, O. Visser, J. G. Snijders, G. te Velde and E. J. Baerends, *Methods and Techniques for Computational Chemistry*, STEF, Cagliari, 1995, 305; (*c*) G. te Velde, F. M. Bickelhaupt, E. J. Baerends, C. Fonseca Guerra, S. J. A. Van Gisbergen, G. J. Snijders and T. Ziegler, *J. Comput. Chem.*, 2001, **22**, 931–967.
15 W. Ravenek, *Algorithms and Applications on Vector and Parallel Computers*, Elsevier, Amsterdam, 1987.
16 G. te Velde and E. J. Baerends, *J. Comput. Phys.*, 1992, **99**, 84–98.
17 (*a*) J. G. Snijders, E. J. Baerends and P. Vernooijs, *At. Nucl. Data Tables*, 1982, **26**, 483–509; (*b*) P. Vernooijs and E. J. Baerends, *Slater Type Basis Functions for the Whole Periodic System. Internal Report*, Vrije Universiteit of Amsterdam, The Netherlands, 1981.
18 J. B. Krijn and E. J. Baerends, *Fit Functions in the HFS Method. Internal Report (in Dutch)*, Vrije Universiteit of Amsterdam, The Netherlands, 1984.
19 (*a*) E. van Lenthe, A. E. Ehlers and E. J. Baerends, *J. Chem. Phys.*, 1999, **110**, 8943–8953; (*b*) E. van Lenthe, E. J. Baerends and J. G. Snijders, *J. Chem. Phys.*, 1993, **99**, 4597–4610; (*c*) E. van Lenthe, E. J. Baerends and J. G. Snijders, *J. Chem. Phys.*, 1994, **101**, 9783–9792; (*d*) E. van Lenthe, J. G. Snijders and E. J. Baerends, *J. Chem. Phys.*, 1996, **105**, 6505–6516; (*e*) E. van Lenthe, E. J. Baerends and J. G. Snijders, *Int. J. Quantum Chem.*, 1996, **57**, 281–293.
20 A. D. Becke, *Phys. Rev. A*, 1988, **38**, 3098–3100.
21 J. P. Perdew, *Phys. Rev. B*, 1986, **33**, 8822–8824.
22 E. J. Baerends, J. A. Autschbach, A. Bérces, C. Bo, P. M. Boerrigter, L. Cavallo, D. P. Chong, L. Deng, R. M. Dickson, D. E. Ellis, L. Fan, T. H. Fischer, C. Fonseca Guerra, S. J. A. van Gisbergen, J. A. Groeneveld, O. V. Gritsenko, M. Grüning, F. E. Harris, P. van den Hoek, H. Jacobsen, G. van Kessel, F. Kootstra, E. van Lenthe, V. P. Osinga, S. Patchkovskii, P. H. T. Philipsen, D. Post, C. C. Pye, W. Ravenek, P. Ros, P. R. T. Schipper, G. Schreckenbach, J. G. Snijders, M. Solà, M. Swart, D. Swerhone, G. te Velde, P. Vernooijs, L. Versluis, O. Visser, E. van Wezenbeek, G. Wiesenekker, S. K. Wolff, T. K. Woo and T. Ziegler, *ADF2000*, Vrije Universiteit Amsterdam, Amsterdam, The Netherlands, 2000.
23 (*a*) F. M. Bickelhaupt, N. M. Nibbering, E. M. van Wezenbeek and E. J. Baerends, *J. Phys. Chem.*, 1992, **96**, 4864–4873; (*b*) T. Ziegler and A. Rauk, *Inorg. Chem.*, 1979, **18**, 1558–1565; (*c*) T. Ziegler and A. Rauk, *Inorg. Chem.*, 1979, **18**, 1755–1759; (*d*) T. Ziegler and A. Rauk, *Theor. Chim. Acta*, 1977, **46**, 1–10; (*e*) K. Kitaura and K. Morokuma, *Int. J. Quantum Chem.*, 1976, **10**, 325–331.
24 (*a*) C. Fonseca Guerra and F. M. Bickelhaupt, *Angew. Chem., Int. Ed.*, 1999, **38**, 2942–2945; (*b*) C. Fonseca Guerra, F. M. Bickelhaupt, J. G. Snijders and E. J. Baerends, *Chem. Eur. J*, 1999, **5**, 3581–3595; (*c*) C. Fonseca Guerra and F. M. Bickelhaupt, *Angew. Chem., Int. Ed.*, 2002, **41**, 2092–2095; (*d*) J. Poater, X. Fradera, M. Solà, M. Duran and S. Simon, *Chem. Phys. Lett.*, 2003, **369**, 248–255.
25 (*a*) I. Mayer, *Chem. Phys. Lett.*, 1983, **97**, 270–274; (*b*) I. Mayer, *Int. J. Quantum Chem.*, 1984, **26**, 151–154.
26 (*a*) J. Kruszewski and T. M. Krygowski, *Tetrahedron Lett.*, 1972, **13**, 3839–3842; (*b*) T. M. Krygowski, *J. Chem. Inf. Comput. Sci.*, 1993, **33**, 70–78.
27 T. M. Krygowski and M. K. Cyrański, *Chem. Rev.*, 2001, **101**, 1385–1419.
28 P. v. R. Schleyer, *Chem. Rev.*, 2001, **101**, 1115–1117.
29 P. v. R. Schleyer, C. Maerker, A. Dransfeld, H. Jiao and N. J. R. van Eikema Hommes, *J. Am. Chem. Soc.*, 1996, **118**, 6317–6318.
30 K. Wolinski, J. F. Hilton and P. Pulay, *J. Am. Chem. Soc.*, 1990, **112**, 8251–8260.
31 R. F. W. Bader, *Atoms in Molecules: A Quantum Theory*, Oxford University Press, Oxford, UK, 1990.
32 F. Biegler-König, J. Schönbohm and D. Bayles, *J. Comput. Chem.*, 2001, **22**, 545–559.
33 M. J. Frisch, G. W. Trucks, H. B. Schlegel, G. E. Scuseria, M. A. Robb, J. R. Cheeseman, J. A. Montgomery, Jr., T. Vreven, K. N. Kudin, J. C. Burant, J. M. Millam, S. S. Iyengar, J. Tomasi, V. Barone, B. Mennucci, M. Cossi, G. Scalmani, N. Rega, G. A. Petersson, H. Nakatsuji, M. Hada, M. Ehara, K. Toyota, R. Fukuda, J. Hasegawa, M. Ishida, T. Nakajima, Y. Honda, O. Kitao, H. Nakai, M. Klene, X. Li, J. E. Knox, H. P. Hratchian, J. B. Cross, C. Adamo, J. Jaramillo, R. Gomperts, R. E. Stratmann, O. Yazyev, A. J. Austin, R. Cammi, C. Pomelli, J. W. Ochterski, P. Y. Ayala, K. Morokuma, G. A. Voth, P. Salvador, J. J. Dannenberg, V. G. Zakrzewski, S. Dapprich, A. D. Daniels, M. C. Strain, Ö. Farkas, D. K. Malick, A. D. Rabuck, K. Raghavachari, J. B. Foresman, J. V. Ortiz, Q. Cui, A. G. Baboul, S. Clifford, J. Cioslowski, B. B. Stefanov, G. Liu, A. Liashenko, P. Piskorz, I. Komaromi, R. L. Martin, D. J. Fox, T. Keith, M. A. Al-Laham, C. Y. Peng, A. Nanayakkara, M. Challacombe, P. M. W. Gill, B. Johnson, W. Chen, M. W. Wong, C. Gonzalez and J. A. Pople, *Gaussian 03*, Gaussian, Inc., Pittsburgh, PA, 2003.
34 D. Andrae, U. Häussermann, M. Dolg, H. Stoll and H. Preuss, *Theor. Chim. Acta*, 1990, **77**, 123–141.
35 A. W. Ehlers, M. Böhme, S. Dapprich, A. Gobbi, A. Höllwarth, V. Jonas, K. F. Köhler, R. Stegmann, A. Veldkamp and G. Frenking, *Chem. Phys. Lett.*, 1993, **208**, 111–114.
36 P. C. Hariharan and J. A. Pople, *Theor. Chim. Acta*, 1973, **28**, 213–217.
37 C. K. Johnson, *ORTEP, Report ORNL-5138*, Oak Ridge National Laboratory, Oak Ridge, TN, 1976.
38 S. Komeda, M. Lutz, A. L. Spek, Y. Yamanaka, T. Sato, M. Chikuma and J. Reedijk, *J. Am. Chem. Soc.*, 2002, **124**, 4738–4746.
39 S. Komeda, M. Lutz, A. L. Spek, M. Chikuma and J. Reedijk, *Inorg. Chem.*, 2000, **39**, 4230–4236.
40 W. B. Connick, L. M. Henling, R. E. Marsh and H. B. Gray, *Inorg. Chem.*, 1996, **35**, 6261–6265.
41 B.-C. Tzeng, G.-H. Lee and S.-M. Peng, *Inorg. Chem. Commun.*, 2003, **6**, 1341–1343.
42 R. S. Osborn and D. Rogers, *J. Chem. Soc., Dalton Trans.*, 1974, 1002–1004.
43 D. M. Roundhill, in *Comprehensive Coordination Chemistry*, ed. R. D. Gillard, J. A. McCleverty and G. Wilkinson, Pergamon, Oxford, 1987, vol. 5, ch. 52.
44 H. O. Davies, D. A. Brown, A. I. Yanovsky and K. B. Nolan, *Inorg. Chim. Acta*, 1998, **268**, 313–316.
45 C. Mock, I. Puscasu, M. J. Rauterkus, G. Tallen, J. E. A. Wolf and B. Krebs, *Inorg. Chim. Acta*, 2001, **319**, 109–116.
46 M. Mullaney, S.-C. Chang and R. E. Norman, *Inorg. Chim. Acta*, 1997, **265**, 275–278.

47 (*a*) Y. Zhao and D. G. Truhlar, *J. Phys. Chem. A*, 2005, **109**, 5656–5667; (*b*) Y. Zhao and D. G. Truhlar, *J. Chem. Theory Comput.*, 2005, **1**, 415–432.
48 (*a*) P. Belanzoni, M. Rosi, A. Sgamellotti, E. J. Baerends and C. Floriani, *Chem. Phys. Lett.*, 1996, **257**, 41–48; (*b*) T. Ziegler, V. Tschinke and A. Becke, *Polyhedron*, 1985, **6**, 685–693.
49 P. L. Johnson, T. R. Koch and J. M. Williams, *Acta Crystallogr., Sect. B*, 1977, **33**, 1293–1295.
50 (*a*) B. Durham, S. R. Wilson, D. J. Hodgson and T. J. Meyer, *J. Am. Chem. Soc.*, 1980, **102**, 600–607; (*b*) A. W. Cordes, B. Durham, P. N. Swepston, W. T. Pennington, S. M. Condren, R. Jensen and J. L. Walsh, *J. Coord. Chem.*, 1982, **11**, 251–260.
51 P. Flükiger, H. P. Lüthi, S. Portmann and J. Weber, *MOLEKEL 4.0*, Swiss Center for Scientific Computing, Manno, Switzerland, 2000.
52 P. Macchi and A. Sironi, *Coord. Chem. Rev.*, 2003, 238–239, 383–412.
53 P. Popelier, *Atoms in Molecules: An Introduction*, Pearson Education, Harlow, 2000.
54 M. Iwaoka, H. Komatsu, T. Katsuda and S. Tomoda, *J. Am. Chem. Soc.*, 2004, **126**, 5309–5317.
55 W. Koch, G. Frenking, J. Gauss, D. Cremer and J. R. Collins, *J. Am. Chem. Soc.*, 1987, **109**, 5917–5934.
56 (*a*) G. Portella, J. Poater, J. M. Bofill, P. Alemany and M. Solà, *J. Org. Chem.*, 2005, **70**, 2509–2521; erratum; G. Portella, J. Poater, J. M. Bofill, P. Alemany and M. Solà, *J. Org. Chem.*, 2005, **70**, 4560–4560; (*b*) P. A. Kraakman, J.-M. Valk, H. A. G. Niederländer, D. B. E. Brouwer, F. M. Bickelhaupt, W. H. De Wolf, F. Bickelhaupt and C. H. Stam, *J. Am. Chem. Soc*, 1990, **112**, 6638–6646; (*c*) J. E. Gready, T. W. Hambley, K. Kakiuchi, K. Kobiro, S. Sternhell, C. W. Tansey and Y. Tobe, *J. Am. Chem. Soc*, 1990, **112**, 7537–7540; (*d*) S. Grimme, *J. Am. Chem. Soc*, 1992, **114**, 10542–10545; (*e*) G. J. Bodwell, J. N. Bridson, T. J. Houghton, J. W. J. Kennedy and M. R. Mannion, *Angew. Chem., Int. Ed. Engl.*, 1996, **35**, 1320–1321; (*f*) G. J. Bodwell, J. N. Bridson, T. J. Houghton, J. W. J. Kennedy and M. R. Mannion, *Chem. Eur. J.*, 1999, **5**, 1823–1827; (*g*) G. J. Bodwell, J. N. Bridson, M. K. Cyrañski, J. W. J. Kennedy, T. M. Krygowski, M. R. Mannion and D. O. Miller, *J. Org. Chem.*, 2003, **68**, 2089–2098.

